

ORIGINAL RESEARCH

Sustainable Energy

Optimum design and analysis of solar pump with the help of genetic algorithm, a MATLAB tool, and RSM tool at minimum cost

Vineet Singh¹  | Vinod Singh Yadav² | Niraj Kumar³ | Manoj Kumar¹ | Manoj Kumar Singh⁴

¹Department of Mechanical Engineering, School of Engineering and Technology, IFTM University, Moradabad, Uttar Pradesh, India

²Department of Mechanical Engineering, NIT Uttarakhand, Pauri Garhwal, India

³Department of Electronics and Communication Engineering, Jaypee Institute of Technology, Noida, India

⁴Department of Mechanical Engineering, MJP Rohilkhand University, Bareilly, Uttar Pradesh, India

Correspondence

Vineet Singh, Department of Mechanical Engineering, School of Engineering and Technology, IFTM University, Moradabad, Uttar Pradesh, India.

Email: vineetpsh@gmail.com

Abstract

In this research paper, a well-performing solar pump at the minimum cost of project life is designed and installed. Initially, the capacity of submersible pumps and discharge have been determined based on the water requirement of the crop and the size of the field. The total number of solar panels, inverter size, and motor pump system have been designed based on the law of conservation of energy. The two optimization techniques genetic algorithm (GA) and response surface methodology (RSM) have been used for analyzing the pump performance parameters and total cost. The GA tool has been used to determine the optimum tilt angle on which responses namely solar flux, solar panel efficiency, exergy, and pump efficiency should be maximum. Moreover, the performance of the solar pump at the optimum tilt angle has been compared with the 28° fixed tilt angle (latitude of location). For the experimental study solar pump experimental setup of 5 hp power has been installed in Faculty of Engineering and Technology, MJP Rohilkhand University at 28.36°N, 79.43°E. The total cost of the solar pump has been optimized with the help of RSM based on the discharge and head of the solar pump. The new optimization approach reduced the levelized cost of electricity (LCOE) from 0.041 to 0.035 \$/kWh and the payback period is reduced from 4 to 3 years. The annual increment in average solar flux and overall efficiency has been recorded to be from 606 to 697 W/m² and 11% to 14% respectively.

KEYWORDS

exergy, genetic algorithm, head and discharge, optimization, RSM, solar pump, tilt angle

1 | INTRODUCTION

The photovoltaic water pumping system would give the right path in agriculture to improve the revenues of the farmers by reducing the cost of irrigation. In the future, people will be considered agriculture as an opportunity for employment due to increased profit due to the use of solar pumps operated by photovoltaic (PV) modules. The PV modules included 80% cost of the initial investment in the solar pump

but due to drastically reduction of solar panel costs from 1970 to 2013 was 76.7 to 0.74 \$,¹ which is very economical to the farmers. Power production by PV modules is very popular in recent times due to its multiple benefits. A floating PV module technology reduced the 85% levelized cost of the energy (LCOE) and reduces the evaporation of water in rivers.² The simulation of the solar pump at maximum power point tracking (MPPT) with a vanadium redox flow battery (VRFB) gives the smooth characteristic curve of current, voltage, and

torque.³ The two sensors controller has tracked the Sun energy in a very efficient way.⁴ The daily discharge of the solar pump has been optimized by maximizing the solar pump efficiency at full day, for that MPPT system is used in between the PV module and the inverter minimizes the mechanical and electrical losses by operating the system on the field control.⁵

The head developed by the solar pump has been maximized by increasing input energy supplied by solar panels in two locations in Croatia and Osijek.⁶ The economic feasibility of the PV and diesel-operated pump have been checked and model comparison was done based on power capacity at different locations and different conditions of the environment.⁷ The solar panel and diesel generator reduced the considerable amount of LCOE.⁸ The solar water pumping system and the existing system run by conventional energy sources have been economically tested in the Faculty of Engineering and Technology (FET) in Jamia Millia and concluded that the total cost of the solar photovoltaic (SPV) system is around 10 lac that will return in 4 years payback period. However, the total life of the pump was 20 years then it will supply the water for up to 16 years without spending any cost. It will also save the cost of 3 lac per year which was an early spend for running the conventional diesel-operated pump.⁹ The economic feasibility of three PV arrays of size (1040, 1400, and 1750 W) with conventional diesel engines have been compared in remote areas of Sahara Africa. The average yearly flow rate and cost of PV array sizes were 60 m³/day and 0.04 \$/m³.¹⁰

The experimentation on a 610 Wp, PV generator under different environmental conditions has been performed in which a total of 10% electrical losses have been reduced.¹¹ A financial study on the solar pump operated by a photovoltaic module has been carried out for knowing the effect of financial factors (initial investment, internal rate of return, cost of water discharge, depreciation with time, and the income tax benefit) in the economic analyses. The evaluation results concluded that the higher-cost solar pump is not viable for potential India.¹² The 130 types of solar pumps have been installed and studied in eight states of Mexico which were of few kW to 2 kW. This study provides big data for the financial study of solar pump technology and gives a comparison between PV technology with the traditionally used methods of irrigation.¹³ Solar pump technology has been used in place of diesel engines for calculating annual savings in fuel costs. They found a reduction in the amount of CO₂ and cost due to the installation of the solar photovoltaic pump in India. They concluded that if the daily solar flux supplied was 5.5 kWh/m² for a 1.8 kW solar photovoltaic pump then the total cost saving will be 405.06 \$/ton as compared to diesel fuel.¹⁴ The experimental and simulation results on solar photovoltaic pumps have been compared with 5% accuracy.¹⁵

A solar pump has been designed according to the size of the land to be irrigated and crop water evapotranspiration. They used dynamic simulation for determining the demand and supply of water.¹⁶ The crop evapotranspiration is an important factor in agriculture. In this paper, the experimental and numerical results of seasonal groundwater were validated with a lysimeter a tool for measuring groundwater evapotranspiration.¹⁷ The simulation results have been validated economically with the experimental results on the selected site by several

mathematical models.¹⁸ A hybrid power station operated by wind and solar energy was experimentally validated with the simulation results.¹⁹ A method has been developed for performance prediction of a solar pump located in the St. Catherine area, South Sinai, and Egypt's climatic conditions. The design of the system was based on a minimum supply of discharge per day of 8 m³ and 30–40 m head to be developed by the pump. For performance prediction computer simulation was used. He finally concluded that the efficiencies of PV array in winter and summer were 13.86% and 13.91%, respectively.²⁰ Based on available data, the empirical relationship has been developed. This empirical relation is further used for getting the beam, diffuse, reflected radiation on the horizontal and inclined surface.²¹ A case study has been presented on the use of solar pumps in agriculture and livelihood as compared to conventional fuels like diesel and gasoline.²² A standard frequency converter (FC) has been used in place of the inverter on the solar pump system due to cost savings.²³

They numerically and experimentally examine the effect of nano-fluid concentration and mass flow rate on the reduction of temperature and efficiency of solar cells.²⁴ The worst month of the year approach has been used for sizing the solar pump and its components. The theoretical results were validated with experimental results on the site aquifer.²⁵ The hybrid optimization multiple energy source (HOMER) tools for simulation has been used on solar pump for a cost comparison. They compared the total net present cost (TNPC) and LCOE on the basis of optimum tilt angle and 45° tilt angle. Finally, they concluded that the TNPC and LCOE values were 32,953 \$ and 0.21 \$/kWh. The total reduction in TNPC values at the annual optimum tilt angle was recorded to be 15.96% with respect to the 45° tilt angle.²⁶

A heat exchanger mounted at the base of the solar plate has been used for improving the performance of the solar plate. The different types of fluids are used for determining the effect of cooling in heat exchangers. The computational fluid dynamics (CFD) tools were used for determining the temperature profile on the solar plate at the varying mass flow rates, solar flux, and ambient temperature conditions. Finally, they concluded that the maximum enhancement in the efficiency of solar panels was recorded to be 17.12% at 1000 W/m² solar irradiance, 45°C ambient temperature, and 0.5 m/s water velocity.²⁷ The solar panel cooling very much affected the performance of the solar panel. A study has been conducted for knowing the performance of solar panels at varying mass flow rates.^{28,29} The exergy of SPWPS has been tested at varying solar flux and ambient temperature and it was only 3.56% at 16 Sx 2P connections of solar panels.³⁰

A standalone SPWPS system has been designed and constructed for irrigating palm trees. The subsystem efficiency was found to be 41% with automatic control of the motor. The system LCOE was 0.141 \$/kWh showing the cost-effectiveness.³¹ The various combination of hybrid energy sources like PV, battery, and diesel engines were studied with load-shifting mechanisms. It was concluded that the best hybrid energy system combination proved to be PV/battery/diesel generator. The cost of energy reduction was recorded to be around 10.70% by the use of a load-shifting mechanism.³² The solar photovoltaic water pumping system (SPWPS) system is very popular in the reason of rainfall having an intensity of 300–400 mm. Moreover, the

TABLE 1 A recent study on the solar pump.

S. No.	Author's details	Description	Year of publication
1	[35]	Multiobjective optimization performed by RSM for hybrid energy source (wind and PV module) with four input variables.	2023
2	[36]	The solar pump performance has been optimized by four important input variables namely power output, head, solar flux, and tilt angle.	2023
3	[37]	Minimizing the number of solar panels by use of an optimization algorithm by adjusting the pump required energy as per the available solar energy.	2023
4	[38]	The PV Syst and Sosit simulation tools have been used for the analysis of solar pumps. The performance of the solar pump is calculated at various tilt angles and finds the optimum tilt angle.	2023
5	[39]	A transformer-less standalone DC/AC converter powered by solar panels. It consists of a cascade boost converter joined with five level inverter. The Cascade Boost converter work on Maximum Power Point Tracking (MPPT) using a fuzzy logic controller.	2023
6	[40]	The study focused on technical and economic surveys in Sub-Sahara Africa. For optimization purposes, HOMER software has been used, and the simulation results determined the LCOE and life cycle cost. The results clearly showed that the diesel-operated pump is not economically sustainable.	2023
7	[41]	The solar pump study was conducted in five different scenarios and these scenarios were classified based on the penalties. The optimum scenario has been selected based on the minimum penalty.	2023

diesel-operated pump has a 300% higher pumping cost as compared to PV operated solar pump.³³ The performance also depends on the elevation since at higher altitudes the atmospheric temperature is lower than the ground level. To prove the worthiness of this statement experiments was performed in Indonesia's high land and low region. Finally, it was concluded that at 1100 meters in height, the pump performed 115% more than the lowland region.³⁴

The above literature review shows that the discharge and total power of the pump depend on the crop water demand and the total head of the pump. Therefore, the size of the SPVWPS depends on the crop of the pump and the head of the pump. In this research paper, the total investment of cost in 2nd order polynomial in terms of discharge and head is developed and represented in the form of contour and surface plots for better clarity. Table 1 represents some recent studies on optimization.

1.1 | Novelty and industrial relevance

The SPWPS system is very much used for supplying water for daily use, irrigation, and in industries, for various purposes. The above literature review shows that the SPWPS performance mainly depends on the three important parameters namely tilt angle, discharge, and head required by the pump. The tilt angle controls the available solar energy at the end of the solar panels and the discharge and head control the performance of the submersible pump. From previous literature, it was also seen that the tilt angle, discharge, and head are the three important parameters on which the overall cost of solar pumps depends. Taking these truths in mind, in this research, a solar pump monthly, seasonal, annual, and three times in a day tilt angle is determined by the genetic algorithm (GA), and the head and discharge are optimized by the response surface methodology (RSM) for minimizing the total cost. This work is novel since the cost function has been determined in terms of

the head and discharge due to that the total cost of the pump can be easily determined by knowing the discharge and head.

2 | METHODOLOGY ADOPTED

The solar panels and submersible pump are the main components of the solar pump. These components contribute 80% of the total cost of the solar pump. For the optimum design of the solar pump, it is necessary to design both components separately. The design of the solar panels is based on solar flux available at that location, tilt angle, and the amount of total power generated.²⁹ The total power generated by solar panels depends on the capacity of the pump, inverter, and pump efficiency. The pump capacity depends on the water required by the crop, the size of the field, and the head required to be developed by the pump.³ So the following methodology is adopted for designing the solar pump presented in Figure 1.

Figure 1 shows the pictorial view of the designing process of all the components of the SPWPS. Initially, with the help of the crop evapotranspiration equation, the discharge or the water required by the pump is determined. In the next step, the pump size has been calculated by the formula $P = \rho g Q h$. The motor size has been calculated by considering the mechanical losses. The inverter size has been calculated by considering the inverter efficiency. Now the number of solar panels have been calculated by applying the law of conservation of energy, the power at the end of the solar panels must be equal to the input power of the inverter.

3 | OPTIMIZATION APPROACH AND DESCRIPTION OF THE MODEL

The two-optimization approach is used to design and estimate the solar pump's performance and cost. The first approach is the GA. GA

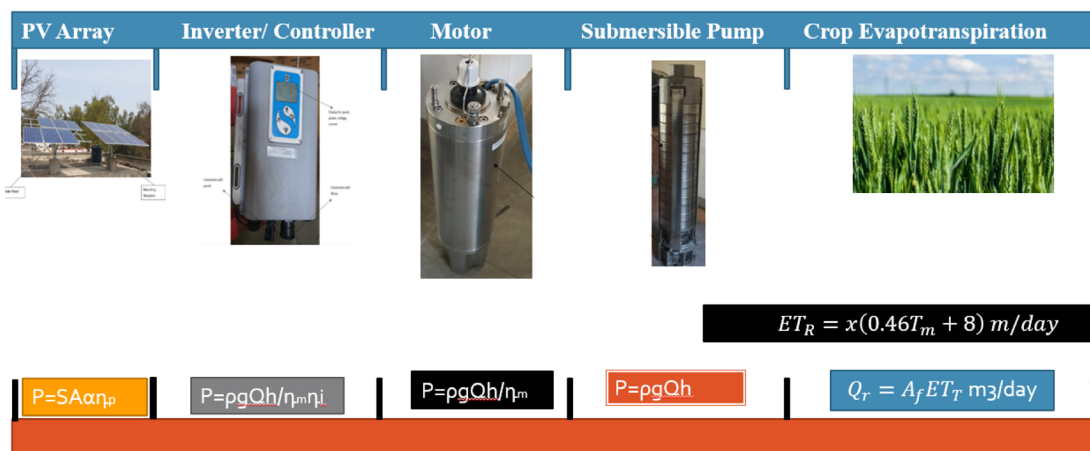


FIGURE 1 Design process of the solar pump.

is used for selecting the number of solar panels based on the maximum solar flux obtained at the optimum tilt angle. As a second approach, the RSM has been adopted to minimize the solar pump cost.

3.1 | Genetic algorithm

GA is used for solving the uncertainty in models for performance prediction.⁴² The GA is based on the natural process of genetics. In this process, in each step algorithm select the parents and produce the child, the selection of parents is based on the constrained equations of the objective function. Finally, the solution is optimized as per the objective function and constrained limit.⁴³

The objective function in the MATLAB GA tool must be minimization type and have less than equality constraints.⁴⁴ It can solve the optimization problem of single and multi-objective functions. Figure 2a,b represent the process of working of GA. Figure 2a shows the steps of working of the GA and Figure 2b shows the more elaborated binary form conversion of various stages in GA. The first step of GA to generate the total population or chromosomes depends on the number of iterations. Second step is to divide and scale the population in the group for crossover and mutation.⁴⁵ The third step is the evaluation of the offspring based on the fitness function or objective function. The next step selects the parents based on fitness function and rejects others to make the population size constant. In this research, the description of the number of parameters used in GA has been presented in Table 2.

The solar irradiation equation is the fitness function that depends on the latitude, hour angle, declination angle, and tilt angle of the solar panel. The latitude of the Bareilly is 28.73° N and for particular days, the declination angle is constant. Therefore, solar irradiation in a day depends on the time of the day and the tilt angle of the solar panel. In this research, our purpose is to find the optimum values of the tilt angle for a particular time of the day to maximize solar irradiation. The other performance parameters like

solar panel efficiency, exergy efficiency, power output, and the efficiency of the pump have been determined at the optimum values of the tilt angle and solar flux.

3.2 | Response surface methodology

RSM is used for the optimization of experimental setup by mathematical regression analysis; it converts the response variables in the form of model equations in terms of input variables. George E. P. Box and Wilson used this method first time in 1951.^{46,47}

The solar pump's total cost mainly depends on the discharge required by the crops and the head required to be developed by the pump. So, in this study, the total cost of the solar pump has been optimized based on the head and discharge of the solar pump. The optimization work has been done in MINITAB-17 software by RSM. The RSM performs the analysis of variance (ANOVA) for regression analysis. Table 2 represents the ANOVA table, which converts the experimental data in the form of statistical model equations of responses in terms of input variables by regression analysis. Based on input variables, the total number of the run is 13.

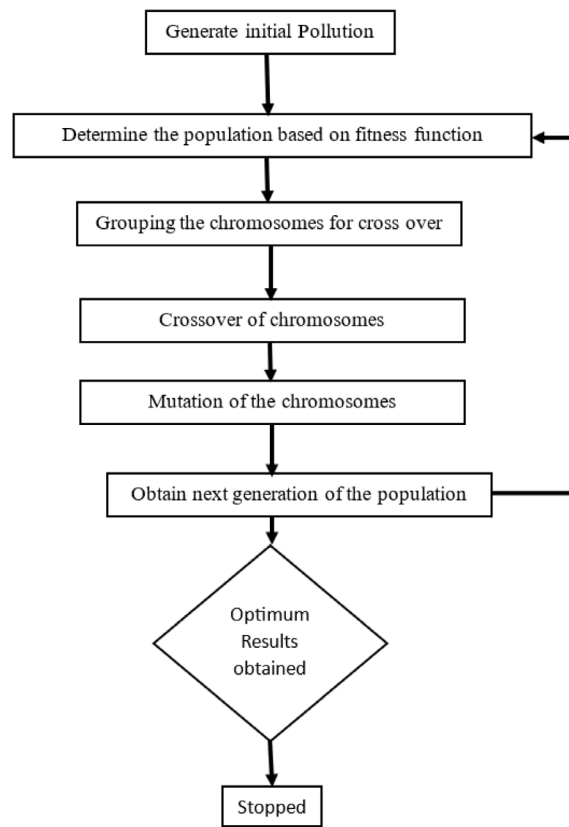
$$\text{Total number of runs are } 2^2 + 2 \times 2 + 5 = 13.$$

After conducting the experiments, the results are analyzed by MINITAB-17 optimization software. Based on inputs and output variables, the second order polynomial of total cost in terms of input variables (discharge and head) has been presented in Equation (1). The model equation generated after regression analyses is given below.

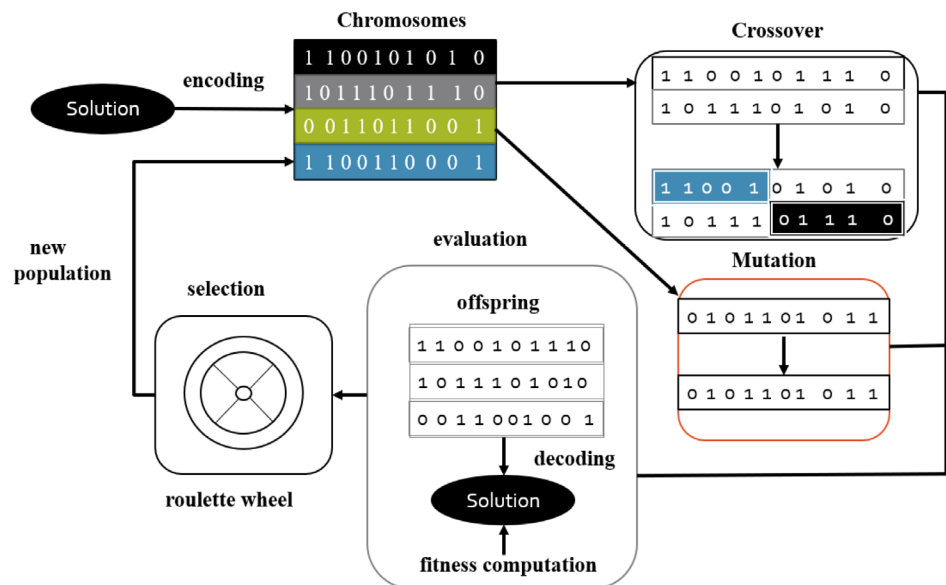
$$C_T(\$) = -0.0126 + 0.00152(Q) - 0.00019(H) + 12.5542QH, \quad (1)$$

where Q is the discharge, H is the head, and C_T is the total cost. The acceptability of the model has been determined based on the S , R^2 , and R^2 (adj) values of the experimental output responses. The S , R^2 , and R^2 (adj) values for C_T are 17.25, 98.12%, and 89.45%. These

FIGURE 2 Steps followed in genetic algorithm (GA).



(a) Steps for the working of GA



(b) Binary form conversion in various stages of GA

obtained values are considerable with good accuracy. Further, the ANOVA accuracy analysis has been calculated based on the F and P value test. The test results of the F value and P value have shown in Table 3 which shows all values of the P test less than 1 that is acceptable. The F values corresponding to the output response parameters are less than 55, so our prediction model based on experimental results is acceptable at a 99% confidence level.

Figure 3 shows the various stages of RSM. In RSM, the first step is to define the input variables and their ranges. These input variables are known as the controlling variables since the responses depend on them. In the 2nd step, define the design of experiments (DoE) matrix which generated the total number of runs at various settings of input variables. Further, with the help of the model equations and experimental work, the responses have been determined. In the next step,

TABLE 2 Genetic algorithm variable.

Population size	150
Algorithm	GA
Cross over rate	70%
Selector	Crowded tournament
Mutation rate	10%
Number of generations	300

TABLE 3 Analysis of variance (ANOVA) for models.

Solar flux					
Source	df	Adj. SS	Adj. MS	F value	p values
Model	5	21.3	22.8	24.65	0.000
Linear	2	16.8	18.9	23.25	0.000
Square	2	15.2	16.5	52.12	0.000
Interaction	1	3.2	3.0	7.24	0.040
Discharge	1	1.9	1.89	24.29	0.001
Head (m)	1	1.7	1.7	5.2	0.000
Q ² H	1	1.65	1.8	3.2	0.0001

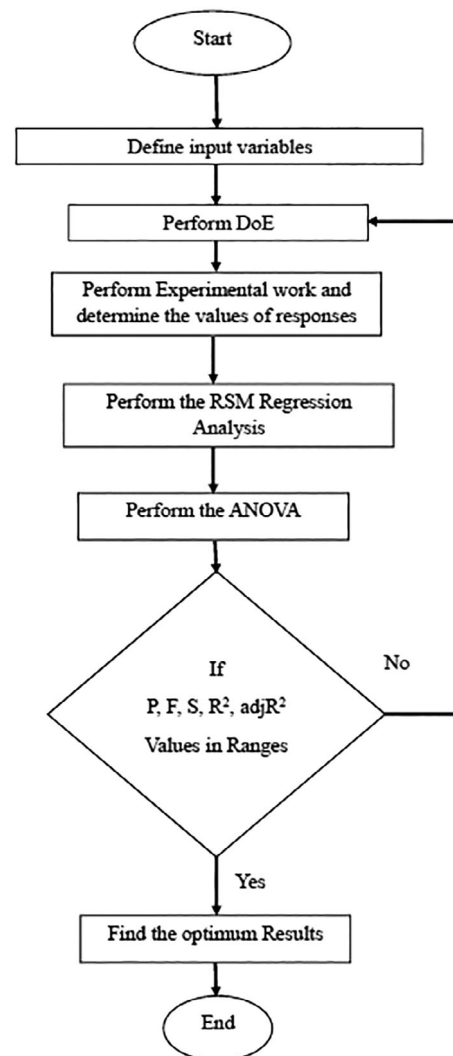
ANOVA performs regression analysis and generates the values of P , F , S , R^2 , and $\text{adj}R^2$ values. Based on these parameters model accuracy has been tested and then the surface and contour graphs have been plotted.

4 | MODEL EQUATIONS FOR SOLAR PHOTOVOLTAIC WATER PUMPING SYSTEM

The dynamic simulation of the solar photovoltaic water pumping (SPWP) system required the mathematical modeling of solar panels, inverter, pump, crop water demand, and total cost. The PV plate model is based on the law of conservation of energy. The total solar energy available on a solar module is absorbed, converted into electricity, and remains wasted in the atmosphere. The DC power generated by the solar panels is controlled and supplied for the submersible pump with the help of an inverter. The crop water demand model is required to fulfill the water demand of the crop as well as be used for designing the submersible pump. The submersible pump model depends on the optimum discharge and head required to be developed. The cost model is based on net present value (NPV) and LCOE. It is used for the calculation of the payback period and cost of production of one unit of electricity.

4.1 | PV module

The work of PV modules is to convert solar energy into electric power. The electric energy generated by PV modules depends on the angle of tilt, surface azimuth angle, and the size of the solar panels. The radiation reached on the surface of the PV module is the contribution of three parts: beam radiation, diffuse radiation, and reflected radiation.

**FIGURE 3** Flow diagram of working of response surface methodology (RSM).

The total radiation on a tilted surface is given by the following equation represented in Reference [48].

$$\frac{H_t}{H_g} = \left(1 - \frac{H_D}{H_g}\right) R_b + \frac{H_D}{H_g} R_d + R_r \quad (2)$$

where H_t monthly average daily global radiation on a tilted surface (kWh/m^2 day), H_g monthly average daily global radiation on a horizontal surface (kWh/m^2 day), H_D total diffuse radiation and R_b , R_d , and R_r are the beam, diffuse, and reflected radiation factors. The value of $\frac{H_D}{H_g}$ is further calculated by an equation represented in Reference [48].

$$\frac{H_D}{H_g} = 1.411 - 1.696 \left(\frac{H_g}{H_0}\right) \quad (3)$$

where H_0 monthly average daily extra-terrestrial radiation on a horizontal surface (kWh/m^2 day). The value of $\frac{H_g}{H_0}$ is determined by equation.⁴⁹

$$\frac{H_g}{H_o} = a + b \left(\frac{S}{S_{\max}} \right), \quad (4)$$

where a , and b are the constants depending on the location of the place described in Reference [49] and S , S_{\max} is the day length, maximum day length depends on the sunrise and sunset angle. The tilt factors are depending on the solar geometry and inclination of the panel from horizontal. Beam tilt factors equations are presented in Reference [21].

$$R_b = \frac{w_{st} \sin(\delta) \sin(\phi - \beta) + \cos(\delta) \cos(\phi - \beta) \sin(w_{st})}{w_s \sin(\phi) \sin(\delta) + \cos(\phi) \cos(\delta) \sin(w_s)}, \quad (5)$$

$$R_D = \frac{1 + \cos(\beta)}{2}, \quad (6)$$

$$R_r = \rho \left[\frac{1 - \cos(\beta)}{2} \right]. \quad (7)$$

The first law and second efficiency models are also required for the thermal analysis of solar panels. The first law efficiency of the solar panel is given by Reference [21].

$$\eta_{pv} = \frac{V_m I_m}{I_t A}, \quad (8)$$

where V_m , I_m are the maximum voltage and current generated by solar panels, I_t is the insolation received on solar panels (W/m^2) and A is the area of the solar panels (m^2).

The exergy balance equation for the solar panel is given by the equation

$$E_{X_{in}} - E_{X_{out}} = E_{\text{destruction}}, \quad (9)$$

where $E_{X_{in}}$ is the exergy supply to the solar panel, $E_{X_{out}}$ is the exergy leaving the solar panel and $E_{\text{destruction}}$ is exergy destroyed due to irreversibility present in the system.

The $E_{X_{in}}$ is given by Reference [13].

$$E_{X_{in}} = A I_t \left[1 - \frac{4}{3} \left(\frac{T_a}{T_{\text{Sun}}} \right) + \frac{1}{3} \left(\frac{T_a}{T_{\text{Sun}}} \right)^4 \right], \quad (10)$$

where T_a , T_{Sun} is the atmospheric and sun temperature in Kelvin (K).

The exergy $E_{X_{out}}$ is the combination of two parts one is the electrical exergy and 2nd is the exergy loss in the atmosphere due to high temperature.

$$E_{X_{out}} = E_{x_{el}} + E_{x_{atm}}. \quad (11)$$

The $E_{x_{el}}$ is the electrical work and given by

$$E_{x_{el}} = V_m I_m. \quad (12)$$

The $E_{x_{atm}}$ is given by Reference [14]

$$E_{x_{atm}} = (h_c + h_r) A (T_m - T_{\text{Sky}}) \left(1 - \frac{T_a}{T_m} \right), \quad (13)$$

where h_c is the convection heat transfer coefficient (W/m^2K).²⁶

$$h_c = 2.8 + 3v, \quad (14)$$

where v is the velocity of air flowing over the solar PV module. h_r is the radiation heat transfer coefficient.²⁶

$$h_r = \epsilon \sigma (T_{\text{Sky}} + T_m) (T_{\text{Sky}}^2 + T_m^2). \quad (15)$$

The energetic efficiency calculation gives the real performance of the solar panel system. The exergetic efficiency is the ratio of the exergy recovered to the exergy supplied. The exergy recovered is the electricity generated by the solar panel and the exergy supplied is the total exergy reached on the solar panels. So exergetic efficiency is represented by the equation shown below.

$$\psi = \frac{V_m I_m}{A I_t \left[1 - \frac{4}{3} \left(\frac{T_a}{T_{\text{Sun}}} \right) + \frac{1}{3} \left(\frac{T_a}{T_{\text{Sun}}} \right)^4 \right]}. \quad (16)$$

Figures 4 and 5 represent the theoretical calculation of power output from the solar panels and the exergy calculation.

4.2 | Inverter-pump model equations

Figure 6 shows the different heads in the submersible pump. The total dynamic head against which the pump is worked is given by the following equation.

$$H_{\text{Total}} = H_g + H_{\text{static}} + H_{\text{Drawdown}} + H_{\text{friction}}, \quad (17)$$

where H_g is the height of the water tank from the ground level, H_{static} is the height difference between the ground and the water level when the pump is not operating, H_{Drawdown} is the head difference between the water level and head reduction due to the operation of the pump and H_{friction} is the frictional head loss.

The frictional head loss is given by the following equation

$$H_{\text{friction}} = \frac{(fL + \sum K) V^2}{2g}, \quad (18)$$

where f is the friction factor, L is the pipe length, D is the pipe diameter, g is the gravitational acceleration and $\sum K$ is the sum of minor head loss factor and V is the velocity of the water.

Now pumping power required to pump the water

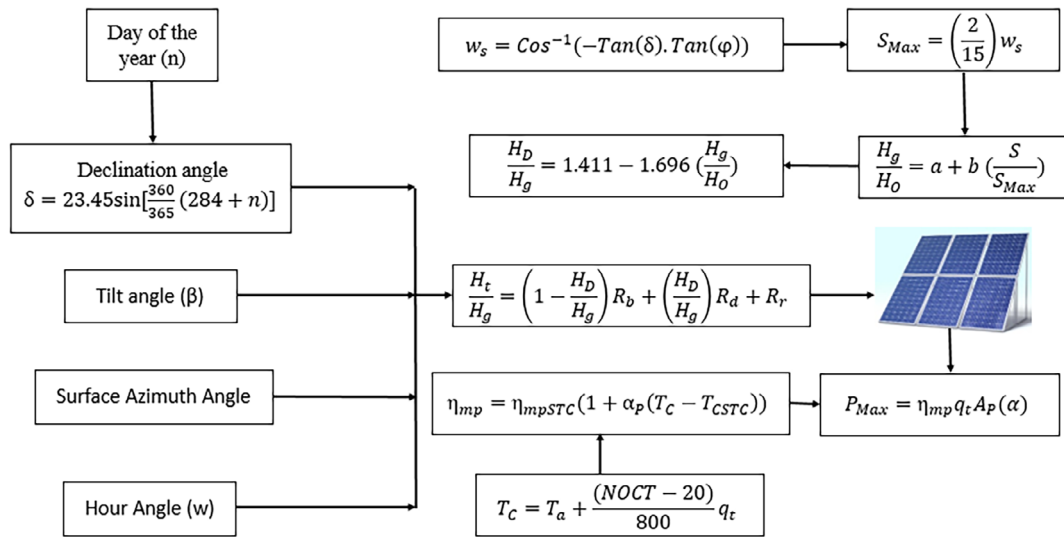


FIGURE 4 Pictorial view of theoretical calculation of power out from solar panels.

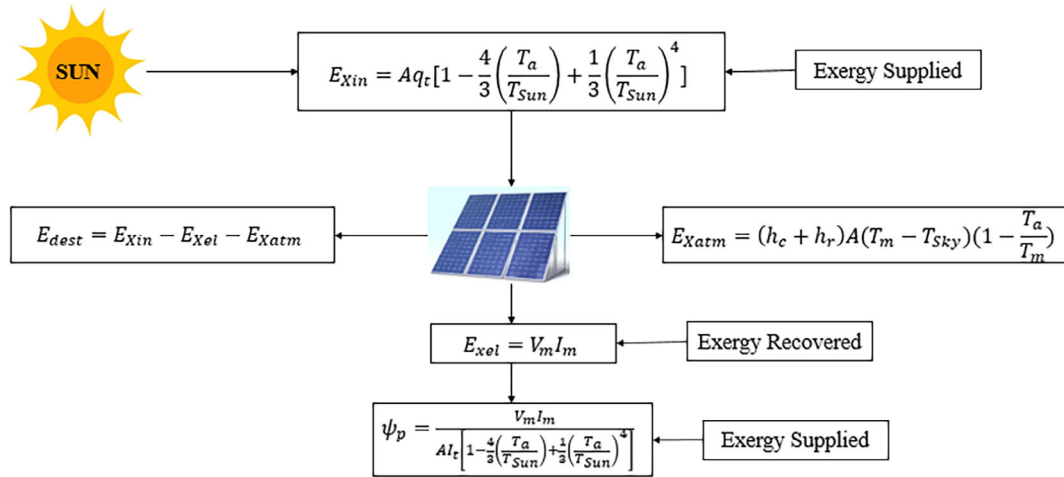


FIGURE 5 Pictorial view of theoretical analysis of exergy calculation.

$$P = \rho g Q H_{Total} \tag{19}$$

So, the pump efficiency

$$\eta_m = \frac{P}{P_m} \tag{20}$$

where P_m is the motor's electric power supply. Now the overall efficiency of the system given by

$$\eta_o = \eta_m \eta_p \tag{21}$$

The borehole drawdown is a very important parameter. It is calculated by the following equation in the PV-SYST software modeling.

$$H_{Total} = \frac{QH_{Totalref}}{Q_{ref}} \tag{22}$$

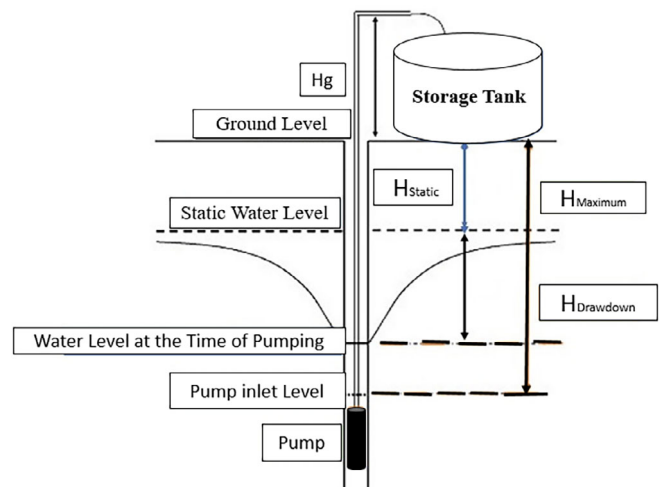


FIGURE 6 Different heads in submersible pump.

where $\frac{H_{\text{Totalref}}}{Q_{\text{ref}}}$ is considered as the specific drawdown having a unit of (m/m³/h), the specific drawdown depends on the discharge of the pump. The high discharge represents the high drawdown and required more power for pumping the water. if the drawdown rate is higher than the refilling time of the borehole results in borehole dry-up. So following equation represented, the refilling time. Where A_w is the cross-sectional area of the borehole.

$$t = A_w \left(\frac{H_{\text{Totalref}}}{Q_{\text{ref}}} \right). \quad (23)$$

4.3 | Equations for cost estimation

The first step before investing in any project is to calculate the net present value throughout the life cycle of the project. So-NPV is the difference between the present value of revenue from the project and the net investment in the project. If the value of NPV is positive then the investment in the project is justified otherwise the investment in the project is at risk. It is calculated by the formula given in Reference [26].

$$\text{NPV} = \left(\sum_1^n \frac{\text{CF}_n}{(1+r)^n} - I \right), \quad (24)$$

where CF = cash flow, r = rate of return, n is the number of years of working on a project and I is the investment.

The second factor decides how much cost is incurred for the production of one unit of energy. it is measured by the LCOE.

LCOE is the ratio of the total investment up to project life (\$) to the total energy produced by the project (kWh).²⁶

The total investment considers the initial investment, maintenance and operation, and fuel cost.

$$\text{Total investment up to project life} = \sum_0^n \frac{I_t + M_t + F_t}{(1+r)^n}, \quad (25)$$

$$\text{Total energy produced by the project in its life time} = \sum_0^n \left(\frac{E_t}{(1+r)^n} \right), \quad (26)$$

$$\text{Now finally LCOE} = \frac{\sum_0^n \frac{I_t + M_t + F_t}{(1+r)^n}}{\sum_0^n \left(\frac{E_t}{(1+r)^n} \right)}, \quad (27)$$

where I_t is the initial investment, M_t is the maintenance & operation cost, F_t is the fuel cost, r is the discount rate, n is the number of years and E_t is the energy produced in project life. The unit of LCOE is the \$/kWh, which shows the cost of production of one unit of energy. it is mainly used for comparison of the different project's economic viability, the project which has the least value of LCOE will be preferred.

5 | EXPERIMENTAL SET-UP OF A SOLAR PUMP LOCATED AT 28.36°N AND 79°E IN INDIA

Figure 7 represents the full schematic diagram of the solar pump setup located at 28.36°N and 79.43°E, at FET, MJP Rohilkhand University, Bareilly. A total of 15 modules have been used in the system and all modules are connected in series as represented in Figure 8. The solar panels, controller, submersible pump, suction, and delivery pipe are the main components of the SPWPS. The solar panel converts the solar energy into the direct current (DC) and the controller converts the DC into an alternating current (AC). The controller is the essential part of

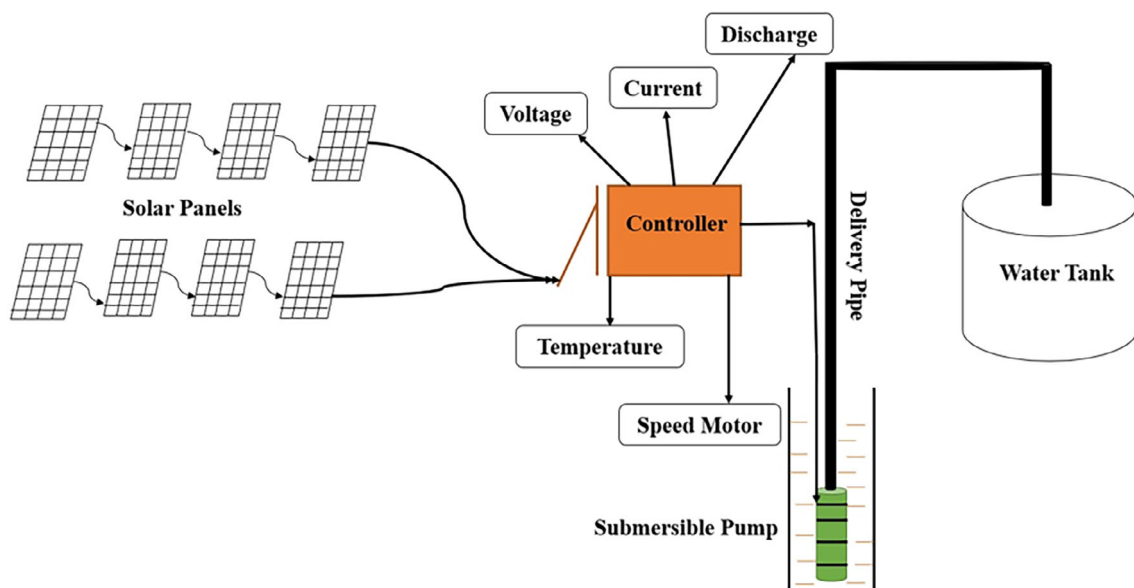


FIGURE 7 Schematic diagram of solar photovoltaic water pumping system (SPWPS).



FIGURE 8 Photovoltaic (PV) array structure.

the solar pump, which is provided with a liquid crystal display (LCD) display. The display shows the reading of the current, voltage, and temperature of the solar panes as well as the pump discharge, speed of the motor, and head developed by the pump. All components of the solar pump, the specification of the PV module, the specification of the controller, the specification of measuring instruments, and the accuracy of the device are given in Reference [50].

For increasing the revenue of farmers, the solar pump project is used for supplying the water of a 0.25 ha farm for irrigation, and the remaining time is used for supplying power to the grid. The 5 hp pump used for irrigation of a 0.25 ha farm, the 3 days' time will be spent for one-time irrigation in a month and the remaining time of the month solar panels will be used for supplying the electricity to the grid. The total time of growing to maturity of the wheat is 120 days of which every month one-time water is required for irrigation. In a year pump remain busy for 36 days for supplying the water and the remaining 353 days will supply the electricity to the grid.

6 | RESULTS AND DISCUSSION

The optimization of the solar pump is completed on the MATLAB GA and RSM tools that give optimized results in terms of tilt angle, maximum solar flux, and minimum cost. The performance of the 5 hp submersible is compared at an optimum tilt angle with a 28° fixed tilt angle (Latitude of the place).

6.1 | Optimized results

6.1.1 | Seasonal optimum tilt angle and annual optimum tilt angle

Figure 9 represents the seasonal variation of the optimum tilt angle with the time of the day. The simulation is completed for four seasons of the year. In the winter season, the optimum tilt angle is 57° which is around two times the latitude of the place. It is observed through the graph the optimum tilt angle is near 90° after 4 p.m.–6 p.m. in the winter season. In the spring season, the

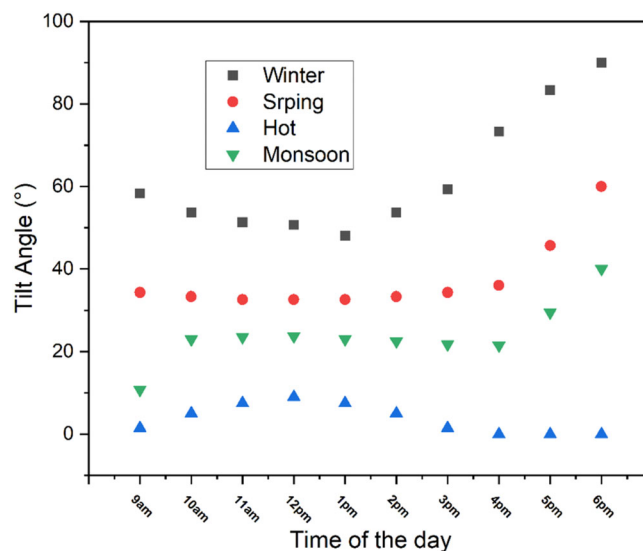


FIGURE 9 Seasonal variation of optimum tilt angle with the time of day.

tilt angle is $(\phi + 9)^\circ$ and varied from 34 to 60° from 9 to 6 p.m. In monsoon season, the average optimum tilt angle is very near to the latitude (ϕ) of the place. It varies from 11° to 40° from 9 a.m. to 6 p.m. In the summer season of May and June, the optimum tilt angle is very less it varies from 2° to 0° from 9 a.m. to 6 p.m., and the average optimum tilt angle throughout the day is around 4°.

Figure 10 represents the annual variation of the optimum tilt angle with the time of the day. From the results, it is identified that the average optimum tilt angle throughout the year maintained is very near to $(\phi + 5)^\circ$ and varies from 27° to 51° from 9 a.m. to 5 p.m. The automatic tracking with the help of the Ordino device²⁷ maintains the optimum tilt angle of the solar PV module so that the sun rays are always perpendicular to the surface of the solar plate. The total cost of the automatic tracking system is 30% more than the manual-operated solar pump.

The seasonal variation of tilt angle three times a day is shown in Figure 11. The seasonal and annual variation of solar tilt angle from 9 a.m. to 6 p.m. by solar tracking system has been seen in Reference [26]. The solar tracking on the single and dual-axis are very costly

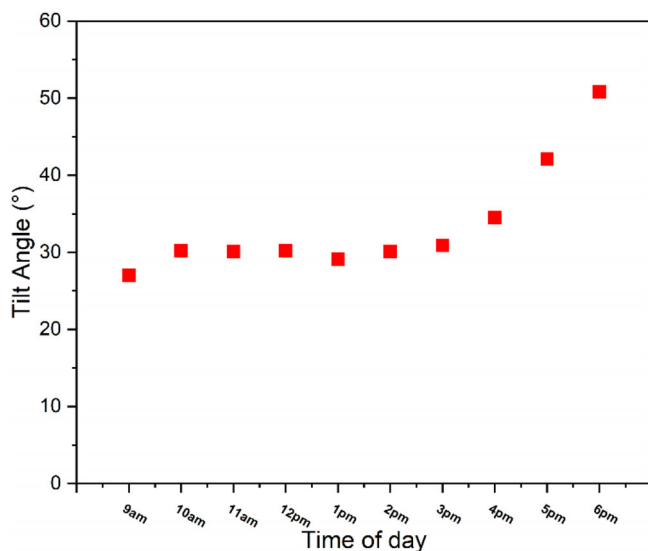


FIGURE 10 Annual variation of optimum tilt angle with the time of day.

and also has a longer payback period. It will increase the initial cost of investment and the maintenance and replacement cost of the solar pump. In this paper, an economical solar pumping system has been designed which has simple and feasible manual tracking on a single-axis at three times of the day in various seasons of the year. The manual tracking is used three times a day at 9 a.m.–11 a.m., 12 p.m.–2 p.m., and 3 p.m.–6 p.m. in four seasons of the year (Summer, spring, monsoon, and winter) as shown in Figure 11. In manual tracking, in a single day, the solar panels are operated three times a day.

The three times in a day one axis manual tracking solar pump is very effective for absorbing the maximum amount of solar radiation at a low cost as presented in Figure 11. In the summer season, the optimum tilt angle should keep 6° from 9 a.m. to 3 p.m. and after 3 p.m. the plate should be kept horizontal. In monsoon season the optimum tilt angle should be kept at 21° , 23° , and 35° from 9 a.m. to 11 a.m., 12 p.m. to 3 p.m., and after 3 p.m., respectively. In the spring season, the optimum tilt angle should be kept at 37° , 33° , and 34° at 9 a.m., 12 p.m., and 3 p.m. respectively.

Figure 12 shows the optimum tilt angle variation annually with the months of the year. The annual tilt angle can be simply changed by mounting the solar panels on the manual tracking stand with rotation about a single axis. The annual manual tracking system has increased the solar flux to 14% as compared to an existing system operated at a 28° tilt angle. It is very simple to operate and its cost is 30% less than the automatic tracking.

6.1.2 | Day and month wise variation of solar flux

Figure 13 shows the variation of solar flux on a daily basis. The overall 14% hike in solar flux is obtained if the system is operated on the optimum tilt angle.

Figure 14 shows the variation of average daily radiation in every month of the year for the 28° tilt angle and the optimum tilt angle.

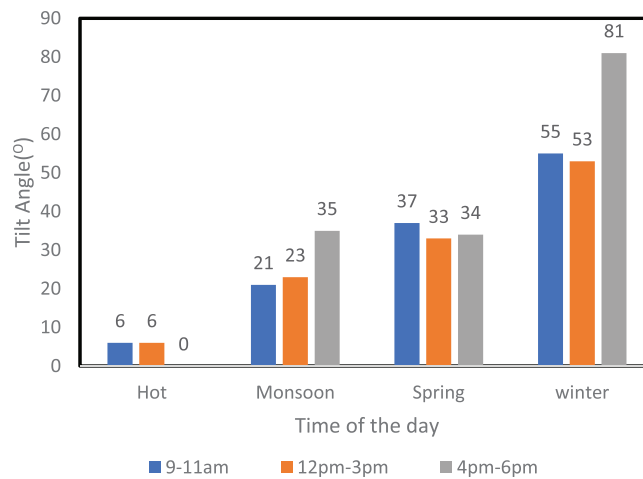


FIGURE 11 Daytime variation of optimum tilt angle at different seasons.

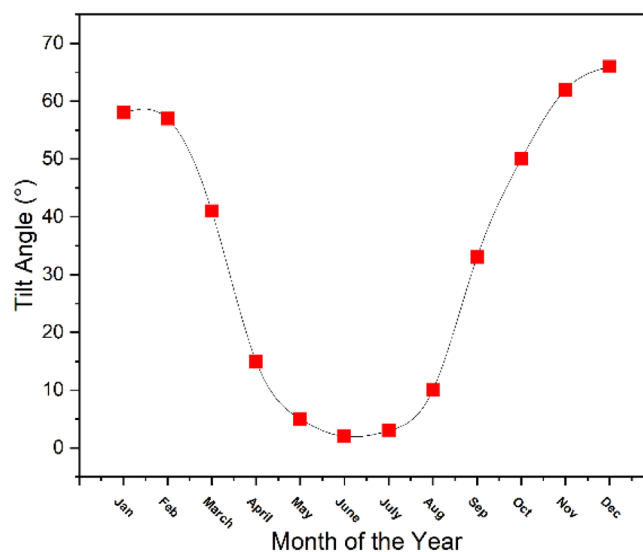


FIGURE 12 Annual variation of tilt angle based on months of the year.

Finally, it is concluded that the daily energy received on the solar panel is higher when the panels are tilted at the optimum angle. The results at the optimum tilt angle show the best performance in October, November, December, January, and February as compared to the 28° tilt angle. The annual increment in the average daily radiation is around 17% due to this new optimization technique.

For the effective working of solar panels, it is necessary to maintain the optimum temperature of solar panels within the nominal operating cell temperature (NOCT).

6.1.3 | Cell temperature and solar panel efficiency variation

As per Figure 15 in May and June, the maximum temperature of the cell is more than 50°C and the NOCT as per Table 2 is 47°C .

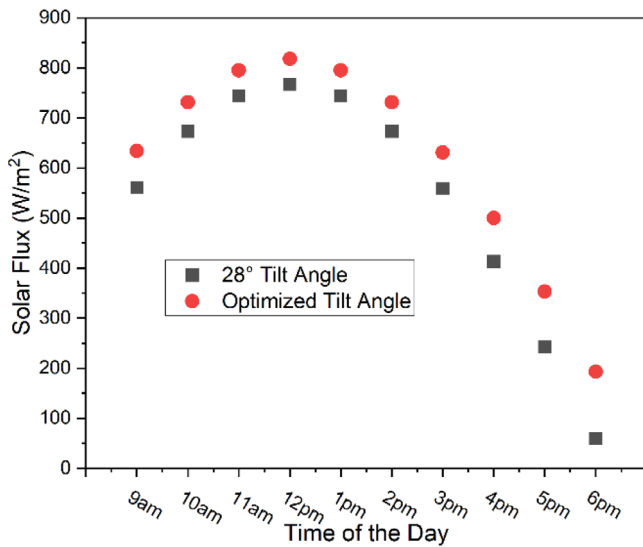


FIGURE 13 Variation of solar flux daily.

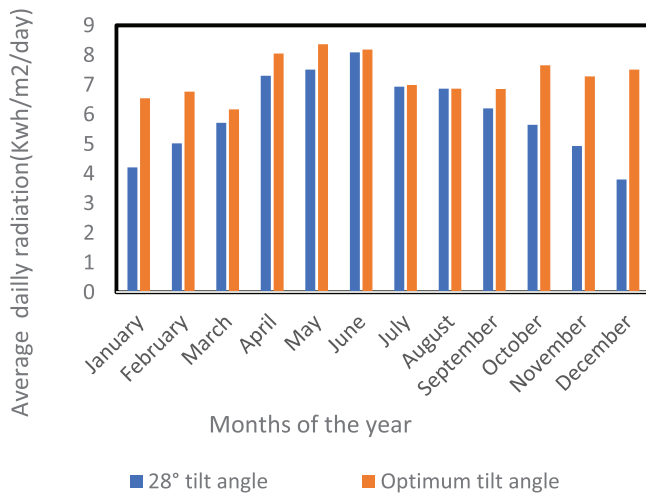


FIGURE 14 Average daily radiation versus months of the year.

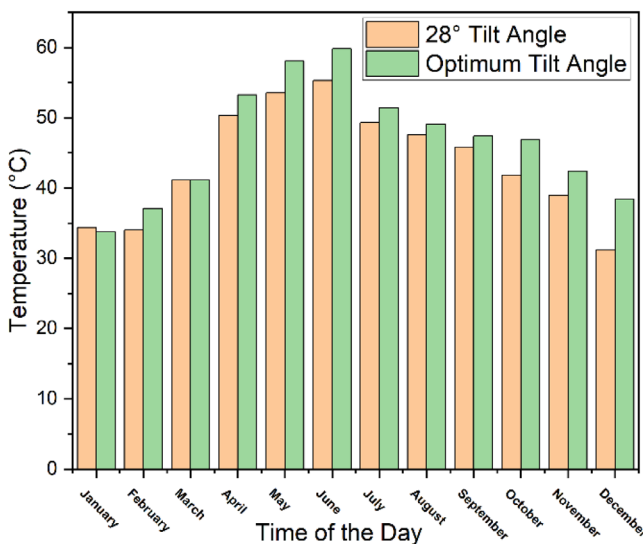


FIGURE 15 Cell temperature based on months of the year.

The higher temperature in May and June reduced the efficiency of solar panels and in other months of the year, the maximum temperature of solar cells is less than 47°C. The optimized results show a little bit higher cell temperature than a 28° tilt angle. It is finally concluded that the optimized system with effective cooling will increase the efficiency of solar panels several times than the 28° tilt angle.

Figure 16 represents the annual average solar panels efficiency to the time of the day. The maximum efficiency of solar panels at a 28° tilt angle is 16% and the maximum efficiency of the solar panel with the optimum tilt angle is 18%. The efficiency of solar panels is minimum at noon and maximum in the morning and evening when the temperature of the solar panel is at the optimum limit.

7 | SOLAR PUMP MODEL VALIDATION

The performance characteristics of the submersible pump have been determined by conducting the test on the pump in the well at the different static heads as shown in Figure 17. At the time of the performance check the discharge of the pump varies from 0 to 15 m³/h, the static head from 15 to 40 m, and the speed of the motor from 30 to 55 Hz. It is observed at the time of experimentation that the system head is continuously increasing and the developed head is continuously reducing with the discharge. Figure 14 shows that it is very difficult for the pump to maintain the developed head at the pump greater than the system head at high discharge (13 m³/h). In such a situation pump will be overloaded and fail. Therefore, it is best for the pump that it will work below the operating point.

At the operating point

$$H_{\text{Required}} = H_{\text{Developed}} \quad (28)$$

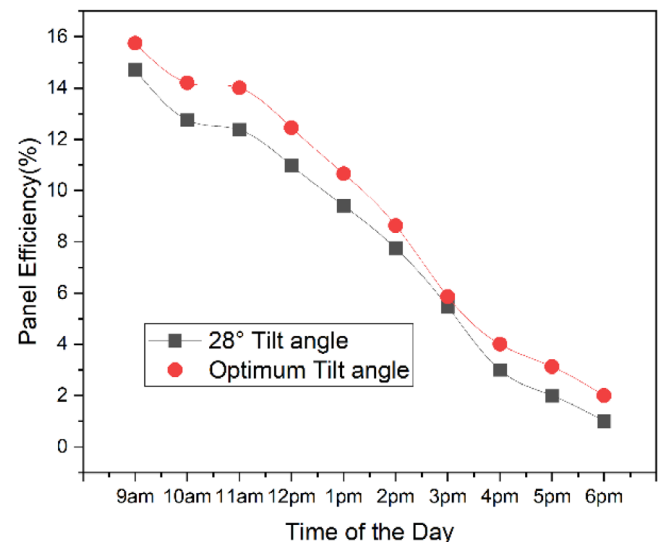


FIGURE 16 Efficiency of solar panel based on months of the year.

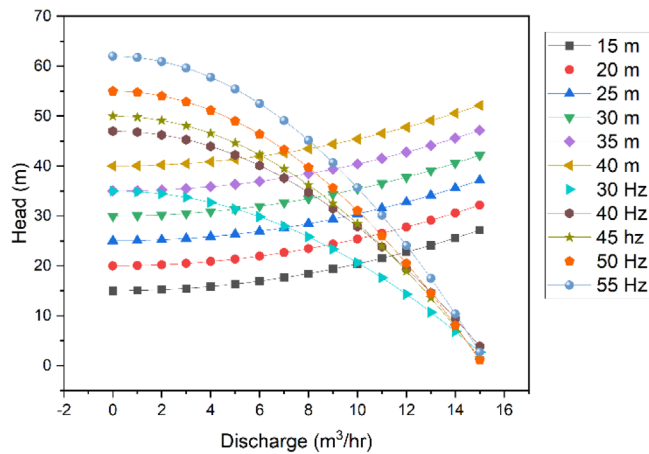


FIGURE 17 The performance curve of a submersible pump operated by an electric supply.

Below the operating point, the developed head by the pump is always greater than the system head (Head required). Figure 17 shows that when the static head varies from 15 to 40 m and the speed of the motor is 30–55 Hz the operating point lies between 10 and 12.5 m³/h. If the discharge in the actual case is in between the given range then pump performance is considered to be the best performance.

The existing solar pump fitted in the borehole has a static head of 35 m and speed variation between 30 and 45 Hz and from Figure 18 the optimum discharge is noted to be 8 m³/h.

7.1 | Pump characteristics curve head and discharge variation in a day operated by PV module

Figure 18 shows the head and discharge variation with the time of the day. The pump will discharge water when the head developed by the pump is greater than the head required by the pump. It is represented in Figure 18 that the existing pump at a 28° tilt angle will discharge the water up to three p.m. and the optimized pump will discharge the water up to 5 p.m. The optimized system gives better head development and discharges as compared to the existing pump at a tilt angle of 28°. In the optimized system and existing system, the discharge up to 1 p.m. is 10 m³/h, it is within the range as explained in Figure 17.

Figure 19 represents that if the power supplied to the motor is less than 890 W_p then the pump will not discharge water.³⁶ The average discharge given by the optimized pump is 9%–11% more than at a 28° tilt angle. The maximum discharge supplied by the optimized pump is 12 m³/h and the 28° tilt angle is 10 m³/h since at the optimum tilt angle PV modules produces more power and the discharge is directly proportional to the power produced by PV modules.⁵⁰ At a low power supply, the difference in the discharge of the optimized system and the existing system running at a 28° tilt angle is very less but at higher power, the difference is high.

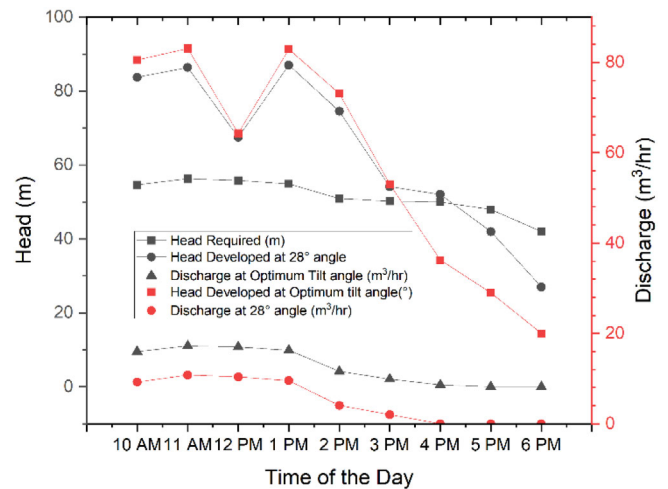


FIGURE 18 Variation of head and discharge throughout the day.

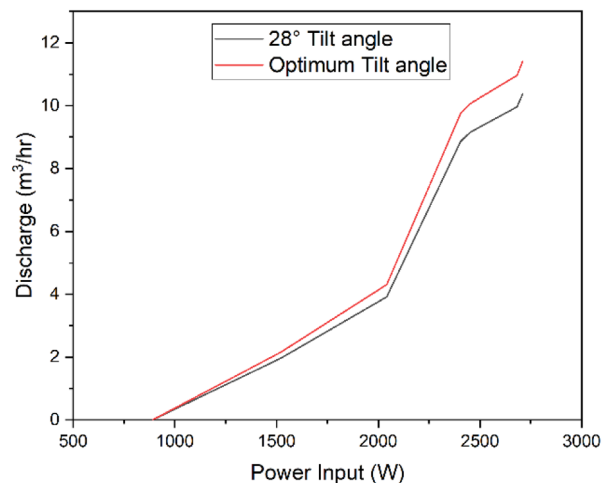


FIGURE 19 Discharge of pump versus power input to motor.

8 | EXERGY ANALYSIS

8.1 | Exergy entering the system

The insolation and exergy received by the solar panel both are maximum at the time of noon as in Figure 20. The optimized system gives the maximum exergy of 22.18 kW at an optimum tilt angle as compared to 20.80 kW at a 28° tilt angle. So exergy received by the optimized system is increased by 7%.

8.2 | Exergy destruction

The exergy destruction as per Equation (9) depends on the temperature difference between the module and the atmosphere. The exergy destruction is increasing in the afternoon and reached a maximum level between 2 p.m. and 3 p.m. in Figure 21.

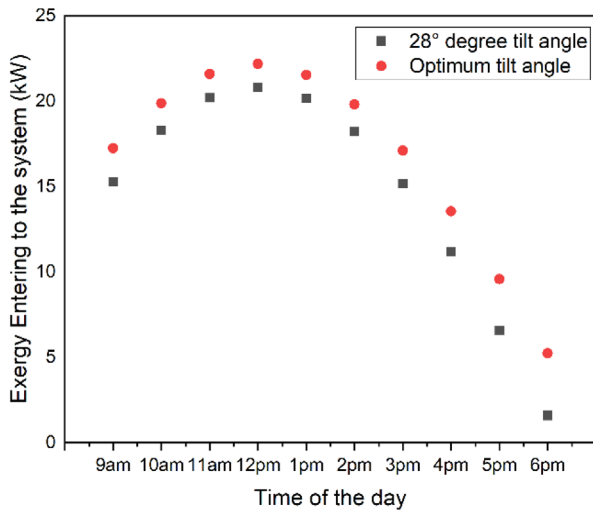


FIGURE 20 Exergy entering the system throughout the day.

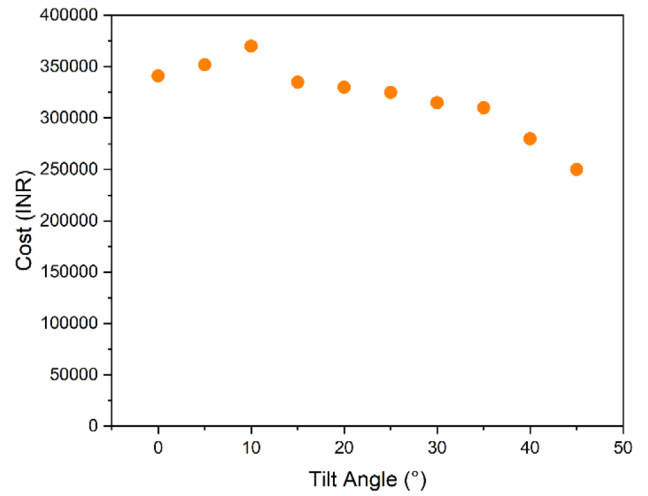


FIGURE 22 Cost variation to the angle of tilt.

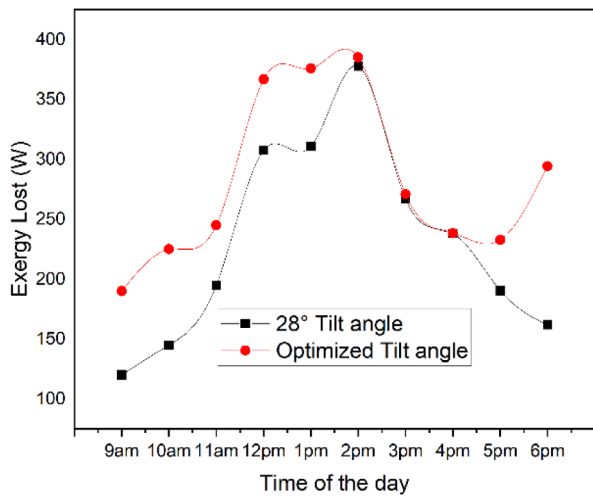


FIGURE 21 Exergy lost to the system throughout the day.

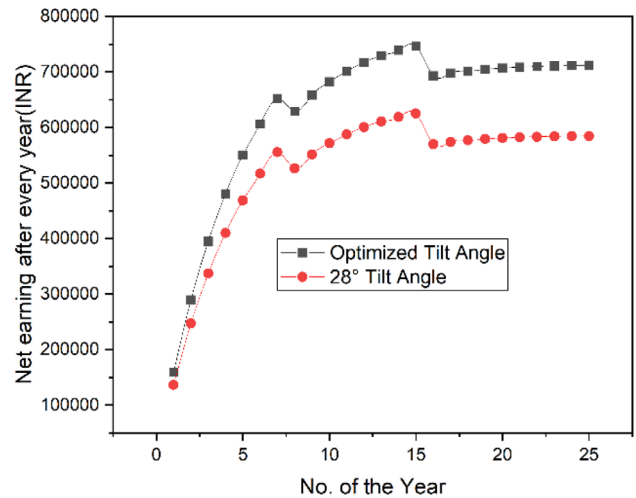


FIGURE 23 Yearwise net earnings on project.

8.3 | Cost model validation

Figure 22 shows the variation of the cost of the solar pump to the angle of tilt. It is identified if the solar pump runs at the annual optimum tilt angle (varies from 27° to 51°) then the total annual cost-saving is 90,000/- on the initial investment as compared to the existing system operating at a 28° tilt angle. Figure 19 represents that the total cost of a solar pump is increasing when the pump operates at less than a 10° tilt angle. So, if the tilt angle will be maintained to be more than 10° then it is beneficial to the farmers.

8.4 | NPV validation

Figure 23 shows the total earnings at the end of the year up to the project life (25 years). If the system will work at the

optimized tilt angle then a net 16% earning will increase in project life as compared to the 28° tilt angle. The NPV of the optimized system is 8456 \$ and in the existing system, 6635 \$ which is operating at a 28° tilt angle. The sudden change in NPV after 8 and 16 years is due to the replacement of the submersible pump and inverter.

8.5 | LCOE and payback period

The LCOE is the money spend in dollars for production of the one unit of electricity, Its unit is \$/kWh. This is a good method of comparison of different ways of production of electricity by different energy sources. If the solar pump runs at the optimum tilt angle then LCOE is reduced from 0.041 to 0.035 \$/kWh in Figure 24. So, a total of 14% cost is reduced due to maintaining the optimum tilt angle on the solar PV module.

The payback period of the optimized system is 3 years and for the existing system run at a 28° tilt angle is 4 years. So overall 33% reduction in the payback period has been achieved due to this new optimization technique. In the case of a 5 hp pump for (0.25 ha), the farmer will recover his investment only in 3 years, and the remaining 22 years of project life can earn 8456 \$.

8.6 | Total cost variation

Figure 25 represents the Pareto chart, which shows the standardized effect of the discharge and head on the total cost of the pump. The value of coefficient α is 0.05, which shows the uncertainty of the results. The results are accurate with 95% accuracy. The

standardized effect of discharge and head are equal in magnitude. The similar standardized effect means the head and discharge are equally responsible for the cost of the solar pump.

Figure 26 shows the 3D representation of the solar pump cost with discharge and head. It is seen that if the pump head and discharge increase, solar pump cost will increase. The cost is directly proportional to the head and the discharge of the solar pump.

Figure 27 shows the contour plot of the total cost of the solar pump with the discharge and head. Figure 27 dark green region shows that if the discharge is higher than 16 m³/h and the head of the pump is higher than 40 m the pump cost will be higher than 8000 \$. The domestic water pump discharge is lower than 8 m³/h due to that its cost is less than 2000 \$ as shown in Figure 27.



FIGURE 24 Levelized cost of energy and payback period.

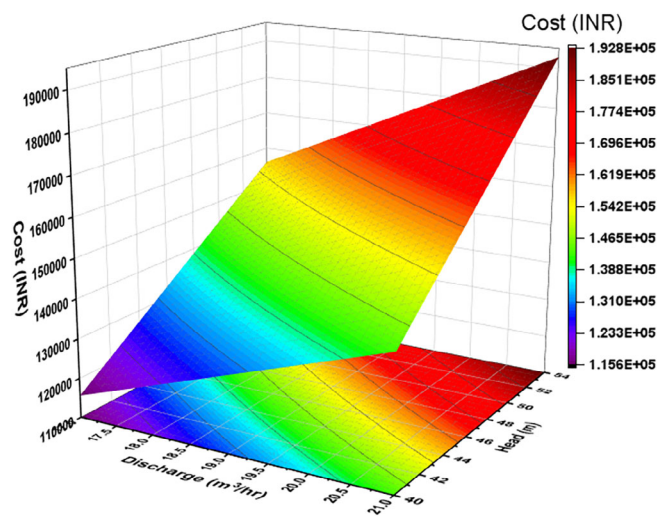


FIGURE 26 Surface plot of the total cost.

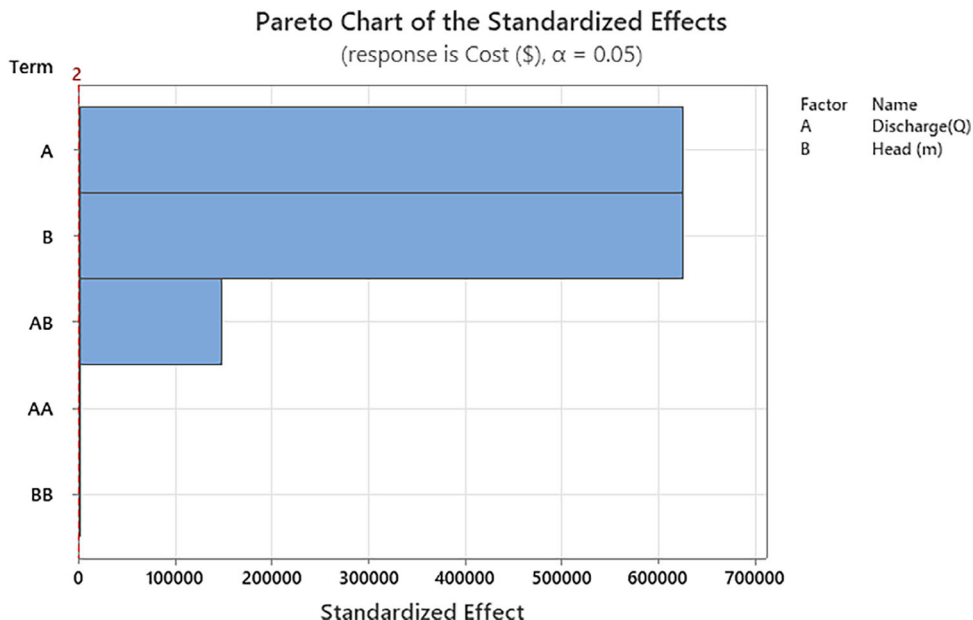


FIGURE 25 Pareto chart of the cost function.

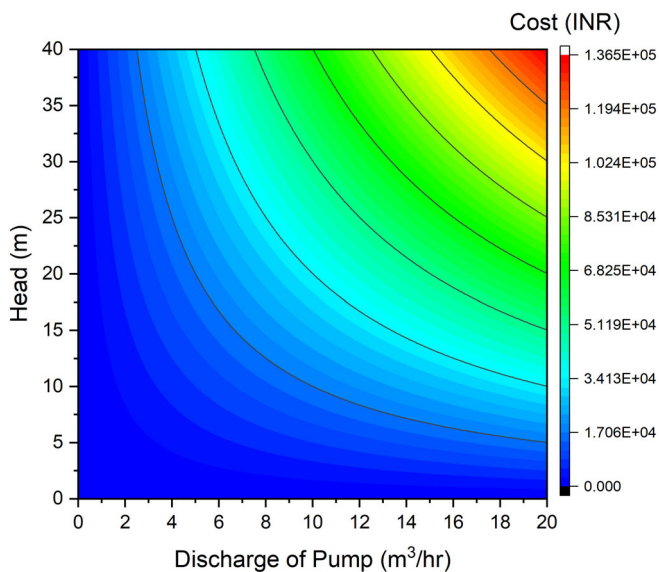


FIGURE 27 Contour plot of the total cost.

9 | CONCLUSION

The new methodology for designing the solar pump based on crop water demand at minimum cost and maximum solar flux give the following concluding points.

1. It is concluded that the optimized system has increased the average solar flux annually from 606 to 697 W/m². The total 15% hike in solar flux is due to running the solar pump at the optimum tilt angle as compared to the 28° tilt angle.
2. The LCOE has been reduced from 0.041 to 0.035 \$/kWh. A total 17% reduction has been recorded in LCOE due to the implementation of this new optimization technique. The reduction in LCOE shows the validity of this new optimization technique. The pay-back period has been reduced from 4 to 3 years, so after 3 years the project will be the source of income for the farmers. A total of 8456 \$ profit has occurred in the project's lifetime.
3. A total of 15 solar panels have been selected due to the use of this new optimization technique. It will supply the optimum discharge at the required head throughout the year. Based on crop water demand and the size of the field (0.25 ha) the capacity of the selected solar pump is 5 hp.
4. The new optimization technique will give the average module temperature within the NOCT (47°C) of the solar panel material throughout the year except for May and June.
5. The above method of designing the solar pump is used only for 0.25 ha. In future work, the same methodology can be used up to 5 ha or more in the size of the field. The main drawback with the solar pump is that due to the increasing size of the field, the size of the solar panels is also increased. So for reducing the size of the solar panels, the solar flux and efficiency of solar panels must be increased, but if the solar flux reached the solar panel enhanced then due to the increase of PV module temperature its efficiency

is reduced. So if an efficient cooling system installed with solar tracking on two axes may improve the solar flux and efficiency of solar panels simultaneously.

6. The total cost of the solar pump in Equation (1) is represented in the form of head and discharge. The discharge and head both are equally responsible for increasing the cost of the solar pump. The total cost model equation has been best fitted with S , R^2 , and R^2 (adj) values of 17.25, 98.12%, and 89.45%.
7. In the ANOVA analysis, the probability of a null hypothesis is 0.05 which shows the statistical data is validated with 95% accuracy.

VARIABLES

a, b	constants
ET_R	reference evapotranspiration (mm/day)
EX_D	exergy destruction due to irreversibility in the system (W)
EX_{IN}	exergy entering in the solar panel (W)
EX_O	exergy leakage in the atmosphere (W)
h_r	radiation heat transfer coefficient W/(m ² K)
h_c	heat transfer coefficient W/(m ² K)
H_d	monthly average daily diffuse radiation on the horizontal surface (kWh/m ²)
H_g	monthly average daily global radiation on the horizontal surface (kWh/m ²)
H_o	monthly average daily extra-terrestrial radiation on the horizontal surface (kWh/m ²)
H_T	monthly average daily radiation on the tilted surface (kWh/m ²)
I_m	maximum current
I_{diode}	diode current (A)
I_L	short circuit current (A)
I_O	reverse saturation current (A)
I_{PV}	total current (A)
K	crop factor
R_S	series resistance (Ω)
S	monthly average of the sunshine hours per day at location (h)
$S_{maximum}$	monthly average of the maximum possible sunshine hours per day at location (h)
T_{sky}	sky temperature (K)
T_{sun}	sun temperature (K)
T_a	atmospheric temperature (K)
T_m	module temperature (K)
V	velocity of airflow over the solar plate (m/s)
V_m	maximum voltage
V_{OC}	open circuit voltage (V)
x	mean daily percentage of annual daytime hours (%)

Greek symbols

ρ	density of water (kg/m ³)
ϕ	exergetic efficiency (%)
σ	Stefan Boltz's man constant (5.67×10^{-8} W/m ² K ⁴)
ε	emissivity of solar panel material

- k Boltzmann constant ($1.38064852 \times 10^{-23} \text{ m}^2 \text{ kg s}^{-2} \text{ K}^{-1}$)
 η efficiency (%)

Acronyms

AC	alternating current
DC	direct current
GA	genetic algorithm
HOMER	hybrid optimization multiple energy source
LCD	liquid crystal display
LCOE	levelized cost of energy
NOCT	nominal operating cell technology
NPV	net present value
PSH	peak sun hour
PV	photovoltaic
RSM	response surface methodology
SPV	solar photovoltaic
SPWPS	solar photovoltaic water pumping system
TNPC	total net present cost

AUTHOR CONTRIBUTIONS

Vineet Singh: Conceptualization; investigation; funding acquisition; writing – original draft; methodology; validation; visualization; writing – review and editing; software; formal analysis; project administration; data curation; supervision; resources. **Vinod Singh Yadav:** Conceptualization; methodology; software; data curation; supervision; resources; project administration; formal analysis; validation; visualization; writing – review and editing; funding acquisition; investigation; writing – original draft. **Niraj Kumar:** Conceptualization; methodology; software; data curation; formal analysis; validation; investigation; funding acquisition; writing – original draft; writing – review and editing; visualization; project administration; resources. **Manoj Kumar:** Writing – original draft; funding acquisition; investigation; conceptualization; methodology; software; data curation; supervision; resources; formal analysis; project administration; validation; visualization; writing – review and editing. **Manoj Kumar Singh:** Conceptualization; funding acquisition; investigation; writing – original draft; writing – review and editing; visualization; validation; methodology; software; project administration; formal analysis; data curation; supervision; resources.

DATA AVAILABILITY STATEMENT

The data that support the findings of this study are available from the corresponding author upon reasonable request.

ORCID

Vineet Singh  <https://orcid.org/0000-0003-3328-2588>

REFERENCES

- Gao Z, Zhang Y, Gao L, Li R. Progress on solar photovoltaic pumping irrigation technology. *Irrig Drain*. 2018;67(1):89-96. doi:10.1002/ird.2196
- Gorjian S, Sharon H, Ebadi H, Kant K, Scavo FB, Tina GM. Recent technical advancements, economics and environmental impacts of floating photovoltaic solar energy conversion systems. *J Clean Prod*. 2021;278:124285. doi:10.1016/j.jclepro.2020.124285
- Bhattacharjee A, Mandal DK, Saha H. Design of an optimized battery energy storage enabled solar PV pump for rural irrigation. Proceedings of the IEEE International Conference on Power Electronics, Intelligent Control and Energy Systems, 2016–2017. doi:10.1109/ICPEICES.2016.7853237
- Abhilash P, Kumar RN, Kumar RP. Solar powered water pump with single axis tracking system for irrigation purpose. *Mater Today Proc*. 2020;39:553-557. doi:10.1016/j.matpr.2020.08.336
- Betka A, Attali A. Optimization of a photovoltaic pumping system based on the optimal control theory. *Sol Energy*. 2010;84(7):1273-1283. doi:10.1016/J.SOLENER.2010.04.004
- Biswas S, Tariq Iqbal M. Dynamic modelling of a solar water pumping system with energy storage. *J Sol Energy*. 2018;2018:1-12. doi:10.1155/2018/8471715
- Odeh I, Yohanis YG, Norton B. Economic viability of photovoltaic water pumping systems. *Sol Energy*. 2006;80(7):850-860. doi:10.1016/J.SOLENER.2005.05.008
- Alhejji A, Kuriqi A, Jurasz J, Abo-Elyousr FK. Energy harvesting and water saving in arid regions via solar pv accommodation in irrigation canals. *Energies*. 2021;14(9):1-24. doi:10.3390/en14092620
- Jamil M, Anees A. SPV based water pumping system for an academic institution. *Am J Electr Power Energy Syst*. 2012;1(1):1. doi:10.11648/j.epes.20120101.11
- Hamidat A. Simulation of the performance and cost calculations of the surface pump. *Renew Energy*. 1999;18(3):383-392. doi:10.1016/S0960-1481(98)00011-1
- Kaldellis JK, Meidanis E, Zafirakis D. Experimental energy analysis of a stand-alone photovoltaic-based water pumping installation. *Appl Energy*. 2011;88(12):4556-4562. doi:10.1016/J.APENERGY.2011.05.036
- Purohit P, Kandpal TC. Solar photovoltaic water pumping in India: a financial evaluation. *Int J Ambient Energy*. 2011;26(3):135-146. doi:10.1080/01430750.2005.9674983
- Foster R, Cisneros G, Hanley C. A cost and reliability comparison between solar and diesel powered pump. Proceedings of the 2nd world conference on photovoltaic solar energy conversion 1998.
- Kumar A, Kandpal TC. Potential and cost of CO₂ emissions mitigation by using solar photovoltaic pumps in India. *Int J Sustain Energy*. 2007;26(3):159-166. doi:10.1080/14786450701679332
- Amer EH, Younes MA. Estimating the monthly discharge of a photovoltaic water pumping system: model verification. *Energy Convers Manag*. 2006;47(15-16):2092-2102. doi:10.1016/J.ENCONMAN.2005.12.001
- Campana PE, Li H, Yan J. Dynamic modelling of a PV pumping system with special consideration on water demand. *Appl Energy*. 2013;112:635-645. doi:10.1016/J.APENERGY.2012.12.073
- Luo Y, Sophocleous M. Seasonal groundwater contribution to crop-water use assessed with lysimeter observations and model simulations. *J Hydrol*. 2010;389(3-4):325-335. doi:10.1016/J.JHYDROL.2010.06.011
- Chahartaghi M, Jaloodar MH. Mathematical modeling of direct-coupled photovoltaic solar pump system for small-scale irrigation. *Energy Source Part A*. 2019;10:1-23. doi:10.1080/15567036.2019.1685025
- Jurasz J, Mikulik J, Krzywda M, Ciapała B, Janowski M. Integrating a wind- and solar-powered hybrid to the power system by coupling it with a hydroelectric power station with pumping installation. *Energy*. 2018;144:549-563. doi:10.1016/J.ENERGY.2017.12.011
- Gad HE. Performance prediction of a proposed photovoltaic water pumping system at South Sinai, Egypt climate conditions. Proceedings of the Thirteenth Water Technology Conference (IWTC 13). Hurgada, Egypt 2009.
- Liu BYH, Jordan RC. The interrelationship and characteristic distribution of direct, diffuse and total solar radiation. *Sol Energy*. 1960;4(3):1-19. doi:10.1016/0038-092X(60)90062-1

22. Foster R, Cota A. Solar water pumping advances and comparative economics. *Energy Proc.* 2014;57:1431-1436. doi:[10.1016/J.EGYPRO.2014.10.134](https://doi.org/10.1016/J.EGYPRO.2014.10.134)
23. Abella MA, Lorenzo E, Chenlo F. PV water pumping systems based on standard frequency converters. *Prog Photovolt Res Appl.* 2003;11(3):179-191. doi:[10.1002/PIP.475](https://doi.org/10.1002/PIP.475)
24. Fayaz H, Nasrin R, Rahim NA, Hasanuzzaman M. Energy and exergy analysis of the PVT system: effect of nanofluid flow rate. *Sol Energy.* 2018;169:217-230. doi:[10.1016/J.SOLENER.2018.05.004](https://doi.org/10.1016/J.SOLENER.2018.05.004)
25. Ebaid MSY, Qandil H, Hammad M. A unified approach for designing a photovoltaic solar system for the underground water pumping well-34 at Disi aquifer. *Energy Convers Manag.* 2013;75:780-795. doi:[10.1016/J.ENCONMAN.2013.07.083](https://doi.org/10.1016/J.ENCONMAN.2013.07.083)
26. Kumar NM, Vishnupriyan J, Sundaramoorthi P. Techno-economic optimization and real-time comparison of sun tracking photovoltaic system for rural healthcare building. *J Renew Sustain Energy.* 2019;11(1):15301. doi:[10.1063/1.5065366](https://doi.org/10.1063/1.5065366)
27. Maleki A, Ngo PTT, Shahrestani MI. Energy and exergy analysis of a PV module cooled by an active cooling approach. *J Therm Anal Calorim.* 2020;141(6):2475-2485. doi:[10.1007/S10973-020-09916-0](https://doi.org/10.1007/S10973-020-09916-0)
28. Belyamin B, Fulazzaky MA, Roestamy M, Subarkah R. Influence of cooling water flow rate and temperature on the photovoltaic panel power. *Energy Ecol Environ.* 2022;7(1):70-87. doi:[10.1007/s40974-021-00223-4](https://doi.org/10.1007/s40974-021-00223-4)
29. Prasad AR, Shankar R, Patil CK, Karthick A, Kumar A, Rahim R. Performance enhancement of solar photovoltaic system for roof top garden. *Environ Sci Pollut Res.* 2021;28(36):50017-50027. doi:[10.1007/S11356-021-14191-Z](https://doi.org/10.1007/S11356-021-14191-Z)
30. Chahartaghi M, Nikzad A. Exergy, environmental, and performance evaluations of a solar water pump system. *Sustain Energy Technol Assessments.* 2021;43:100933. doi:[10.1016/J.SETA.2020.100933](https://doi.org/10.1016/J.SETA.2020.100933)
31. Eltawil MA, Alhashem HA, Alghannam AO. Design of a solar PV powered variable frequency drive for a bubbler irrigation system in palm trees fields. *Process Saf Environ Prot.* 2021;152:140-153. doi:[10.1016/j.psep.2021.05.038](https://doi.org/10.1016/j.psep.2021.05.038)
32. Haffaf A, Lakdja F, Meziane R, Abdeslam DO. Study of economic and sustainable energy supply for water irrigation system (WIS). *Sustain Energy Grids Networks.* 2021;25:100412. doi:[10.1016/j.segan.2020.100412](https://doi.org/10.1016/j.segan.2020.100412)
33. Hilarydoss S. Suitability, sizing, economics, environmental impacts and limitations of solar photovoltaic water pumping system for groundwater irrigation—a brief review. *Environ Sci Pollut Res.* 2021;30:71491-71510. doi:[10.1007/s11356-021-12402-1](https://doi.org/10.1007/s11356-021-12402-1)
34. Sarwono TD, Kusumanto RD. Geographical location effects on PV panel output—comparison between Highland and lowland installation in South Sumatra, Indonesia. *Technol Reports Kansai Univ.* 2021;63(2):7229-7243.
35. Pires ALG, Rotella Junior P, Rocha LCS, Peruchi RS, Janda K, de Miranda RC. Environmental and financial multi-objective optimization: hybrid wind-photovoltaic generation with battery energy storage systems. *J Energy Storage.* 2023;66:107425. doi:[10.1016/j.est.2023.107425](https://doi.org/10.1016/j.est.2023.107425)
36. Waila VC, Sharma A, Singh V, Gupta NK. Solar photovoltaic water pump performance optimization by using response surface methodology. *Environ Prog Sustain Energy.* 2023;42(5):1-14. doi:[10.1002/ep.14148](https://doi.org/10.1002/ep.14148)
37. Lopez-Pascual D, Valiente-Blanco I, Fernandez-Munoz M, Diez-Jimenez E. Theoretical modelling and optimization of a geothermal cooling system for solar photovoltaics. *Renew Energy.* 2023;206:357-366. doi:[10.1016/j.renene.2023.01.098](https://doi.org/10.1016/j.renene.2023.01.098)
38. Habib S, Liu H, Tamoor M, et al. Technical modelling of solar photovoltaic water pumping system and evaluation of system performance and their socio-economic impact. *Heliyon.* 2023;9(5):e16105. doi:[10.1016/j.heliyon.2023.e16105](https://doi.org/10.1016/j.heliyon.2023.e16105)
39. Mohammed MF, Qasim MA, Velkin VI. Stand-alone transformer-less multilevel inverter fed by solar energy for irrigation purposes. *Mater Today Proc.* 2022;80:1071-1078. doi:[10.1016/j.matpr.2022.11.465](https://doi.org/10.1016/j.matpr.2022.11.465)
40. Mulenga E, Kabanshi A, Mupeta H, Ndiaye M, Nyirenda E, Mulenga K. Techno-economic analysis of off-grid PV-diesel power generation system for rural electrification: a case study of Chilubi district in Zambia. *Renew Energy.* 2023;203:601-611. doi:[10.1016/j.renene.2022.12.112](https://doi.org/10.1016/j.renene.2022.12.112)
41. Barbón A, Gutiérrez Á, Bayón L, Bayón-Cueli C, Aparicio-Bermejo J. Economic analysis of a pumped hydroelectric Iberian electricity market. *Energies.* 2023;16(2):1705-1729.
42. Garud KS, Jayaraj S, Lee MY. A review on modeling of solar photovoltaic systems using artificial neural networks, fuzzy logic, genetic algorithm and hybrid models. *Int J Energy Res.* 2021;45(1):6-35. doi:[10.1002/er.5608](https://doi.org/10.1002/er.5608)
43. Yusuf A, Bayhan N, Tiryaki H, Hamawandi B, Toprak MS, Ballikaya S. Multi-objective optimization of concentrated photovoltaic-thermoelectric hybrid system via non-dominated sorting genetic algorithm (NSGA II). *Energy Convers Manag.* 2021;236:114065. doi:[10.1016/j.enconman.2021.114065](https://doi.org/10.1016/j.enconman.2021.114065)
44. Hilali A, Mardoude Y, Essahlaoui A, Rahali A, El Ouanjli N. Migration to solar water pump system: environmental and economic benefits and their optimization using genetic algorithm based MPPT. *Energy Rep.* 2022;8:10144-10153. doi:[10.1016/j.egyr.2022.08.017](https://doi.org/10.1016/j.egyr.2022.08.017)
45. Bouchakour A, Borni A, Brahami M. Comparative study of P&O-PI and fuzzy-PI MPPT controllers and their optimisation using GA and PSO for photovoltaic water pumping systems. *Int J Ambient Energy.* 2021;42(15):1746-1757. doi:[10.1080/01430750.2019.1614988](https://doi.org/10.1080/01430750.2019.1614988)
46. Singh Yadav V, Singh V, Kumar M, Kumar N. Optimization and validation of solar pump performance by MATLAB Simulink and RSM. *Evergreen.* 2022;9(4):1110-1125. doi:[10.5109/6625723](https://doi.org/10.5109/6625723)
47. Singh V, Yadav VS. Optimizing the performance of solar panel cooling apparatus by application of response surface methodology. *J Mech Sci Eng: Part C.* 2022;236(22):11094-11120. doi:[10.1177/09544062221101828](https://doi.org/10.1177/09544062221101828)
48. Glasnovic Z, Margeta J. Optimization of irrigation with photovoltaic pumping system. *Water Resour Manag.* 2006;21(8):1277-1297. doi:[10.1007/S11269-006-9081-8](https://doi.org/10.1007/S11269-006-9081-8)
49. Modi V, Sukhatme SP. Estimation of daily total and diffuse insolation in India from weather data. *Sol Energy.* 1979;22(5):407-411. doi:[10.1016/0038-092X\(79\)90169-5](https://doi.org/10.1016/0038-092X(79)90169-5)
50. Singh V, Yadav VS. Application of RSM to optimize solar pump LCOE and power output. *IETE J Res.* 2022;10:1-25. doi:[10.1080/03772063.2022.2069165](https://doi.org/10.1080/03772063.2022.2069165)

How to cite this article: Singh V, Yadav VS, Kumar N, Kumar M, Singh MK. Optimum design and analysis of solar pump with the help of genetic algorithm, a MATLAB tool, and RSM tool at minimum cost. *Environ Prog Sustainable Energy.* 2023;e14308. doi:[10.1002/ep.14308](https://doi.org/10.1002/ep.14308)